Scanning Microscopy Vol. 11, 1997 (Pages 407-416) 0891-7035/97$5.00+.25
Scanning Microscopy International, Chicago (AMF O'Hare), IL 60666 USA

ELECTRON HOLOGRAPHY: RECENT DEVELOPMENTS

E. Voelkl[1]*, L.F. Allard[1] and B. Frost[2]

[1]High Temperature Materials Laboratory, Oak Ridge National Laboratory, Oak Ridge, TN and
[2]University of Tennessee, Knoxville, TN

Abstract

With the ever increasing speed of modern computers, computing-power hungry applications as electron holography can become more interactive and user friendly and be available for live-time application. New phase unwrapping algorithms and improved reconstruction techniques are discussed together with new approaches to improve the signal/noise ratio in reconstructed phase and amplitude images. While the simplification (from the users point of view) of most routines relays on fast computers and speedy algorithms, the routines for improved signal to noise ratios require not only intensive image processing but automated instrument control as well.

Key Words: Electron holography, reconstruction, signal-noise ratio, phase unwrapping, computer control, automation, remote control.

*Address for correspondence:
Edgar Voelkl
High Temperature Materials Laboratory
Oak Ridge National Laboratory
Oak Ridge, TN 37831-6064
Telephone number: (423) 574-8181
FAX number: (423) 574-4913
E-mail: vog@ornl.gov

Introduction

For the day to day operation of electron holography, particularly in a user facility, it is essential to evaluate holograms rapidly and in a simple manner to access phase and amplitude information not existing in conventionally recorded images.

When looking at an electron hologram, a good part of the information it contains is hidden; the hologram itself appears merely as the regular intensity image (recorded "as usual"), superimposed over fine interference fringes across the image which do not lend themselves to direct interpretation. Therefore, the hologram has to be "reconstructed" to visually display its information. Preferably, the image -or hologram- is recorded digitally, e.g., with a slow-scan charge-coupled device (CCD)-camera and not on film [11].

Unfortunately, the evaluation process can be rather complex requiring the microscopist to concentrate more on the technical aspects of data analysis than the actual object of research. This is due, among other things, to the fact that image processing involving discrete Fourier optics, generally requires special attention to minimize artifacts. It is therefore the software and central processing unit (CPU) which governs how fast and easily accessible the information in the hologram becomes. It should also be mentioned that in order to ensure the reproducibility of results, full information about each processing step should be tied to every image that results from processing.

A Short History

When a slow scan CCD-camera was installed on our Hitachi HF-2000 FEG-TEM (Hitachi, Tokyo, Japan) in March 1993, we were eager for the first holograms from that new camera. Our first digitally recorded hologram was a hologram of small gold particles on amorphous carbon film, which is displayed in Figure 1. The interference fringes in the area of the gold particles (see magnified area) show clearly the strong phase shifting effect of gold, versus the weaker effect of the carbon foil. At that time, we had to use the standard features of DigitalMicrograph for the reconstruction of our holograms, and it was a rather complex and time-consuming

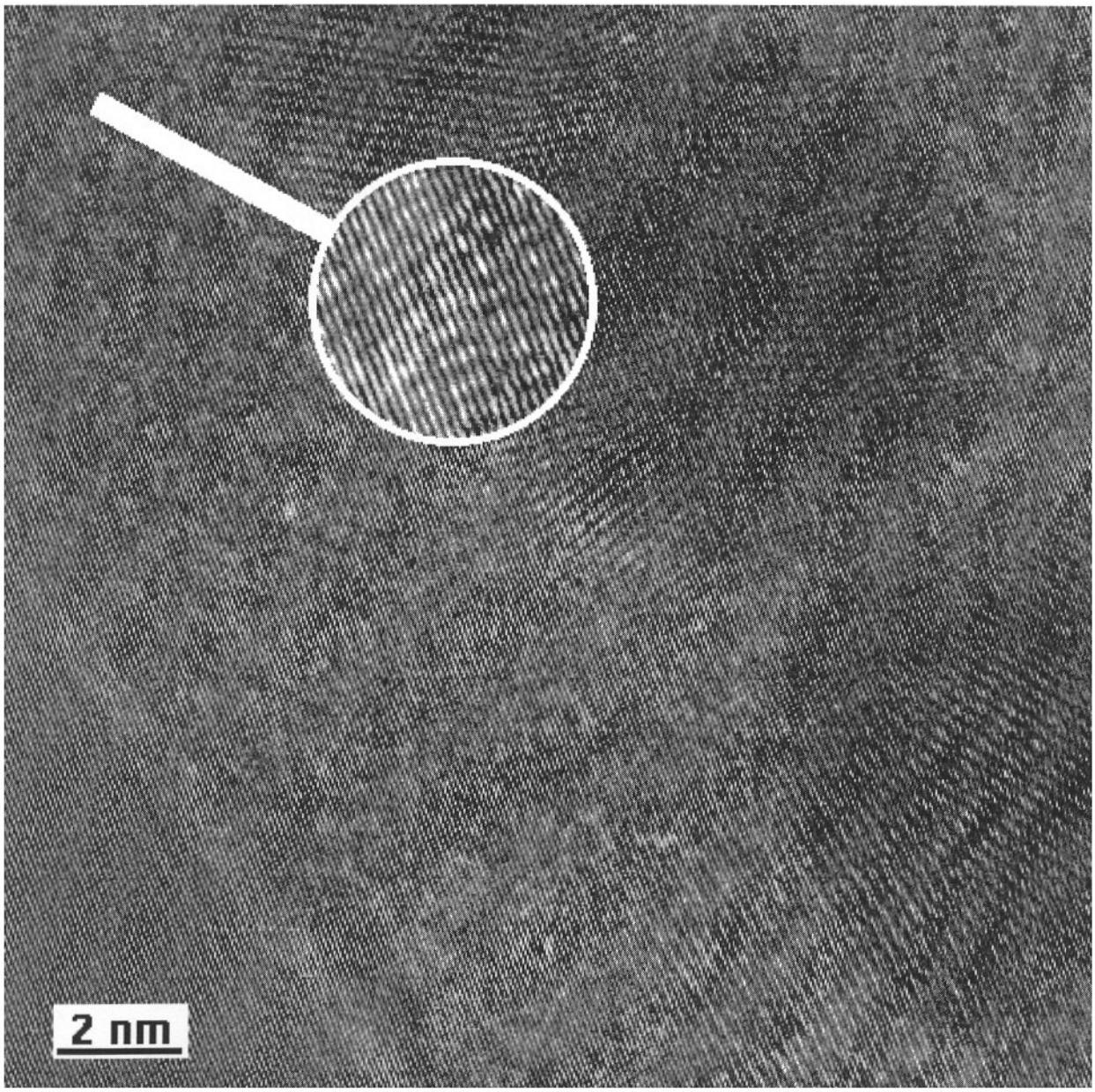

Figure 1. The interference fringes across the gold particles significant fringe bending, while the fringes across the amorphous carbon foil are only weakly modulated.

task before we could actually see the phase image (though still much faster than using film and going through the darkroom first). The speed of a Quadra 950 (the fastest Macintosh available at that time) was not much help either. The total time for the reconstruction of one 1024 by 1024 pixel hologram was about 10 minutes, and clearly, most of the efforts went into the technique itself, which made it difficult to concentrate on the actual sample. These difficulties led to the development of "HoloWorks" software for hologram processing.

More than two years after its first introduction, we are presenting the second version of "HoloWorks" [12]. As the scripting language provided by DigitalMicrograph has improved, and desktop computer speeds have increased, the reconstruction time is now less than 4 seconds on a 225 MHz Macintosh for a 1024 by 1024 pixel image.

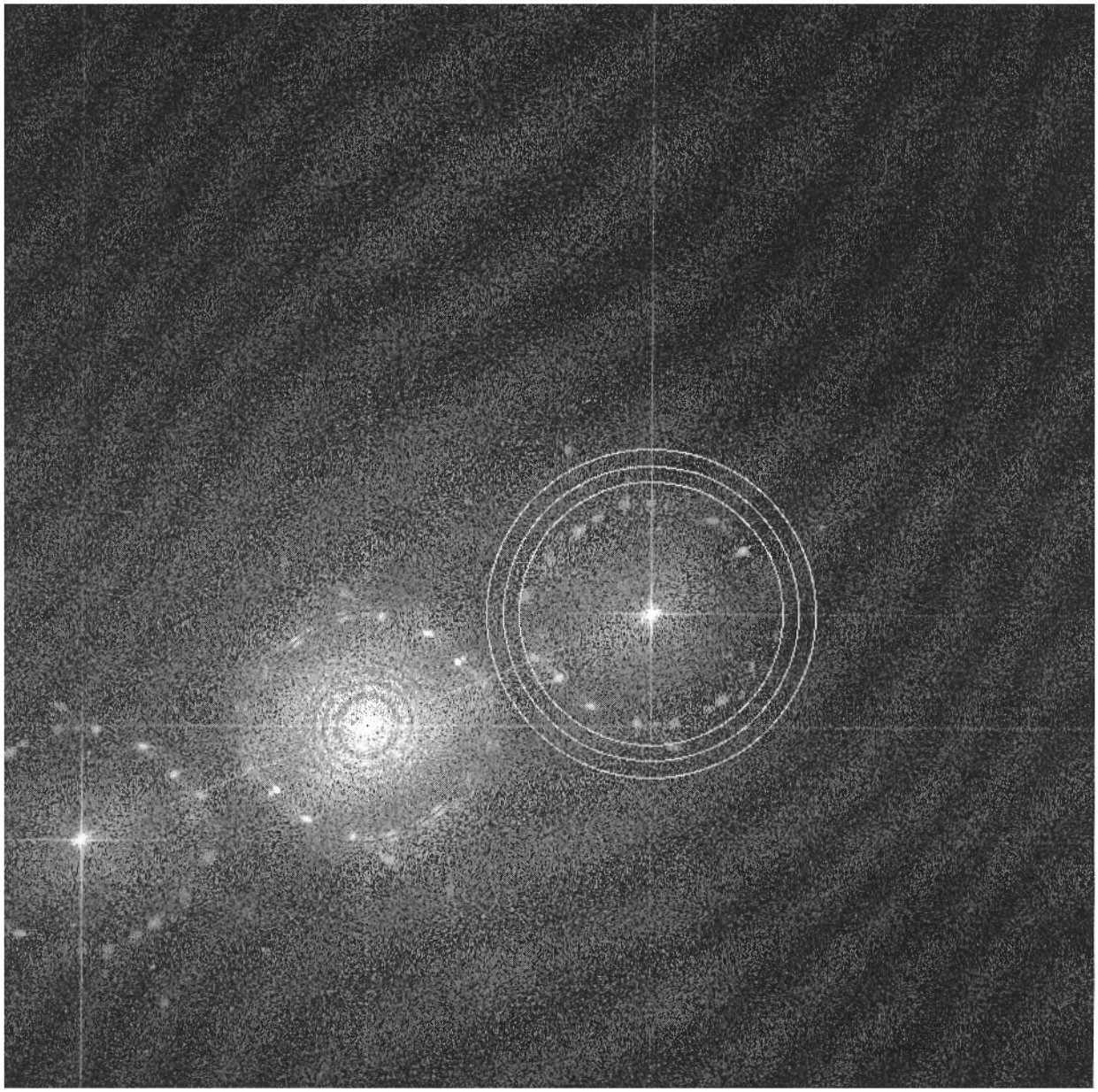

Figure 2. Reconstruction techniques as in HoloWorks 2.0 automatically find the center of the sideband and suggest a (Butterworth) filter to separate the autocorrelation from the sideband. The effective radius as well as the order of the filter can be adjusted interactively.

Automation of the Reconstruction Process

Rapid hologram reconstruction is not only due to fast computers, but also depends on the level of automation. Several levels of automation for the reconstruction of holograms have been developed. There is a fully automatic reconstruction process, where no interaction is necessary (this includes processing with a reference hologram), and phase and amplitude images are reconstructed directly. There is also an interactive reconstruction process, where the user choses two parameters: (a) the size -in comparison to the original hologram- of the reconstructed images and (b) the correct size (and order) of the aperture/filter to be used to separate the sideband from the autocorrelation.

Figure 2 shows the second part of the interactive

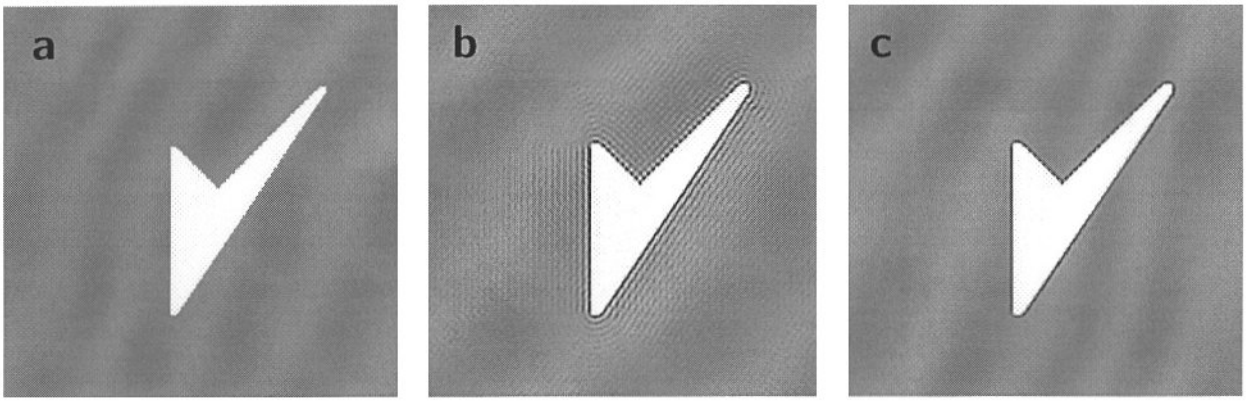

Figure 3. Filtering in Fourier space: (**a**) original, (**b**) after using plane aperture and (**c**) using Butterworth-type (3rd order) aperture. Images were filtered at 1/4 of the Nyquist limit.

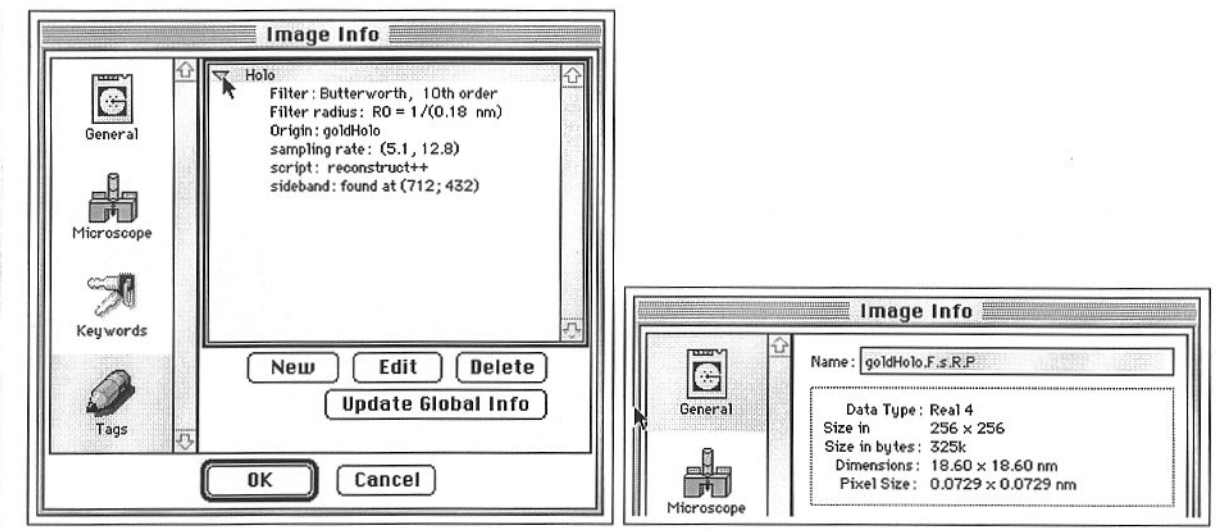

Figure 4. Information on each image is accessible through several windows. Left: the "Tags" window containing information about the reconstruction process and right: the "General" window.

reconstruction process involving a Butterworth filter. The sideband is recognized automatically and the filter, or aperture, separating the sideband from the autocorrelation is already centered on the sideband. The up- and down-arrow keys on the keyboard change the aperture size and the left- and right-arrow keys change the order of the aperture, for a Butterworth filter. The tabular key allows the operator to toggle between a standard aperture with a hard edge and a Butterworth filter.

The Butterworth Filter

As has been discussed in [1, 8, 10], a plain aperture (having a transmission value of 1 inside and 0 outside a given radius) in Fourier space causes artifacts in the reconstructed images, especially if the original hologram is noisy and/or the aperture is small. This is an inherent problem of discrete Fourier optics, where a discrete and limited number of sampling points in real and reciprocal space face a continuum of spatial frequencies in the image. Spatial frequencies which do not coincide with any one of the sampling points in Fourier space display "streaking" which extends along the main axes out to the Nyquist limits. Cutting those streaks by using an aperture with a hard edge can produce severe artifacts in the reconstructed image.

The Butterworth filter is defined as [8]:

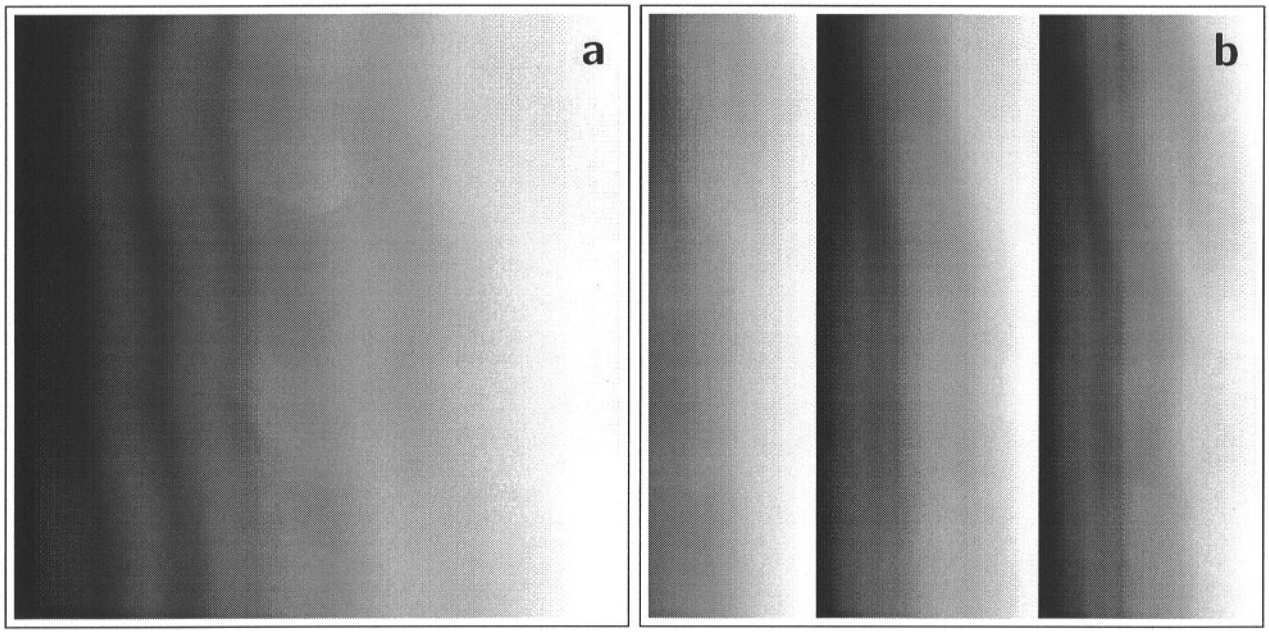

Figure 5. (**a**) An artificial phase image; the phase is increasing linearily from the left to the right. The dynamic range is >2π. (**b**) Same image displayed within [0,2π[resulting in phase jumps.

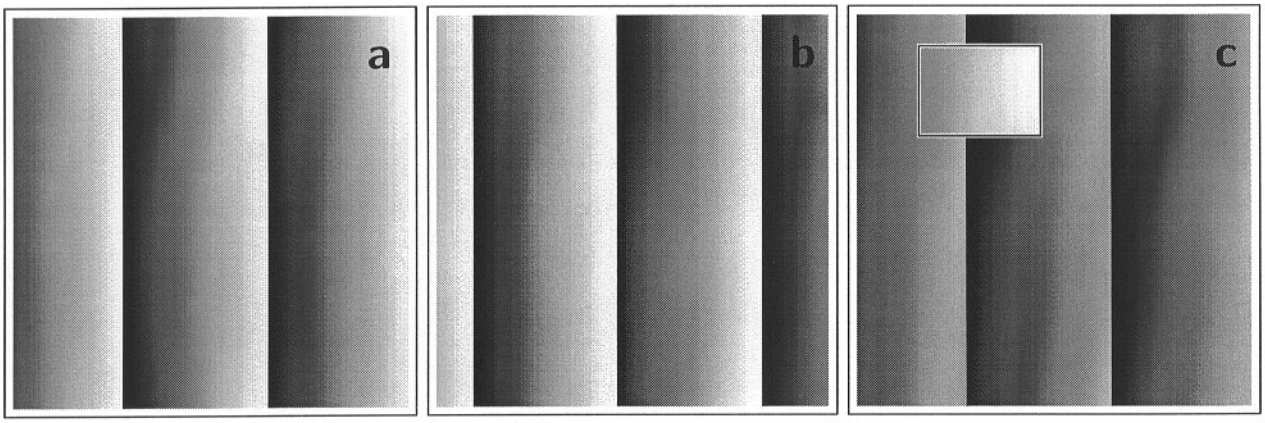

Figure 6. Starting from an image (**a**) with phase jumps and a dynamic range of [0, 2π[, a second image (**b**) can be generated, with a dynamic range [π, 3π[and phase jumps offset by π. Copying an area as outlined in (**c**) from image (**b**) into (**a**) produces image (**c**). Merging (**a**) and (**b**) interactively by carefully moving the selection creates an image with expanded dynamic range an no phase jumps.

$$H = 1 / \{1 + C\ (R/R_0)^{2j}\} \qquad (1)$$

with magnitude H, cutoff value R_0, with R the distance from the center of the filter, C a constant defining H at $H(R = R_0)$ and j the order of the filter.

In Figure 3, an example of the effects of a "hard" aperture versus a "soft" (Butterworth) aperture are displayed. The artificial image in Figure 3a is filtered (low pass) with a hard aperture. As a result, the image in Figure 3b displays smoother corners (due to the filtering), but also shows many artificial fringes around the edges of the original image. In contrast to filtering with a hard filter, the effects of the Butterworth filter are much closer to the desired result: corners and edges are smooth and the presence of artificial fringes is less prevalent. Therefore, the use of high quality filters or apertures is essential for the reconstruction of electron holograms.

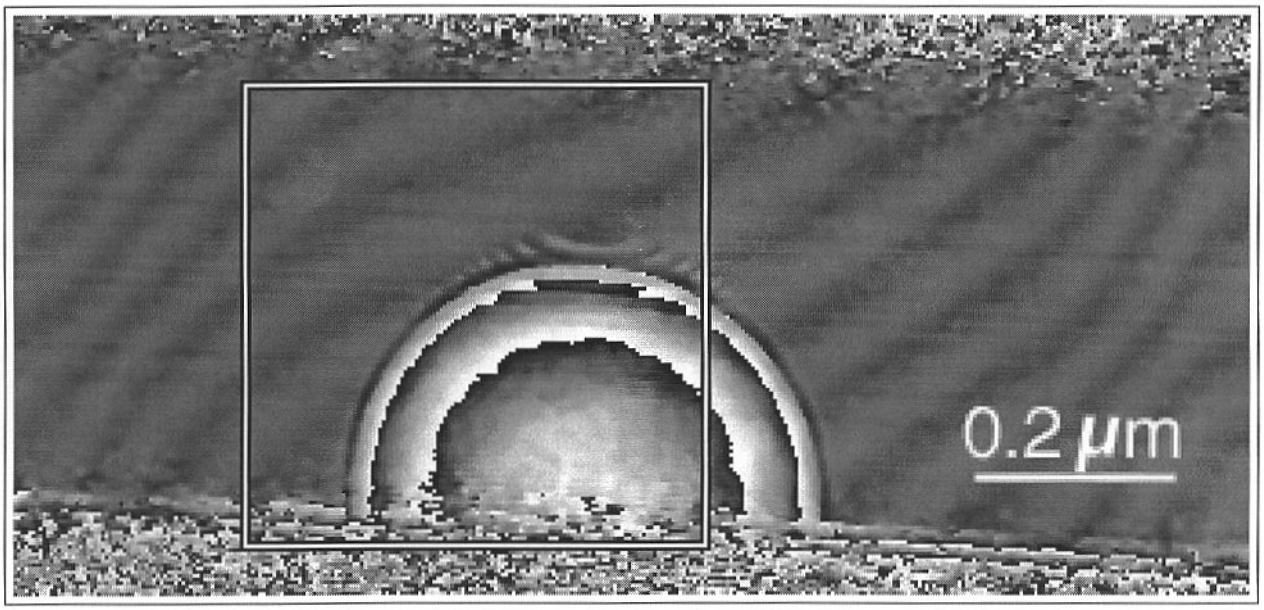

Figure 7. Phase image of a latex sphere (diameter 0.482 µm), as reconstructed using a reference hologram. A slight drift of the biprism causes small remnants of Fresnel fringes (of the biprism) in the vacuum. The area selected is used to align several reconstructed images.

Interactive Reconstruction of Holograms

Once the reconstruction process is started, the software performs a Fourier transform of the image and finds the center of the sideband. An aperture is suggested, centered on the center of the sideband, with a radius corresponding to half the distance between the center of the sideband and the center of the autocorrelation. Unfortunately, the radius and order of the most appropriate filter varies with each hologram and the microscopist is required to make appropriate choices. To simplify the task of selecting the right filter type, the filter is represented by three circles. The outer, middle and inner circles mark the following magnitudes of the filter: 0.1, 0.5 and 0.9 respectively. Once the filter type is selected, the automated reconstruction process continues, and the complex image, the amplitude image and the phase image are finally displayed.

Each reconstruction process evaluates and contains many parameters which need to be stored with the reconstructed images to ensure reproducibility. Each of the reconstructed images carries the full information on the reconstruction steps, and in addition contains information about the name of the original image, the position of the center of the sideband, the sampling frequency for the interference fringes and the reconstruction type used. In case the original hologram was already scaled, all of the reconstructed images are also scaled, and the standard line-tool of DigitalMicrograph can be used to measure distances within those images. The information stored with each image is easily accessible using the "command"-key and "i"-key of the keyboard simultaneously. The use of those keys opens and displays information windows as shown in Figures 4a and 4b.

Phase Unwrapping

Once the complex image Ψ

$$\Psi(x_m, y_n) = A(x_m, y_n)\ \exp[\, i\, \phi(x_m, y_n)] \qquad (2)$$

is reconstructed from a hologram, the image phase $\phi(x_m, y_n)$ can be computed. Unfortunately, any complex image resides on the computer as two real images: the real part ($\Re$) and the imaginary part ($\Im$) of the complex image. Therefore, the phase ϕ of Ψ is computed according to

$$\phi(x_m,y_n) = \arctan2\,[\Re\,(\Psi(x_m,y_n))/\Im\,(\Psi\,(x_m,y_n)] \qquad (3)$$

where arctan2 is a standard C function similar to arctan, but with the full range $]-\pi, \pi[$. This algorithm obviously leads to an ambiguity in the phase image: the phase is determined only modulo 2π and is defined in the dynamic range $]-\pi,\pi[$ (this range is often modified to $[0,2\pi[$ by adding the constant π to the image and taking rounding errors into account).

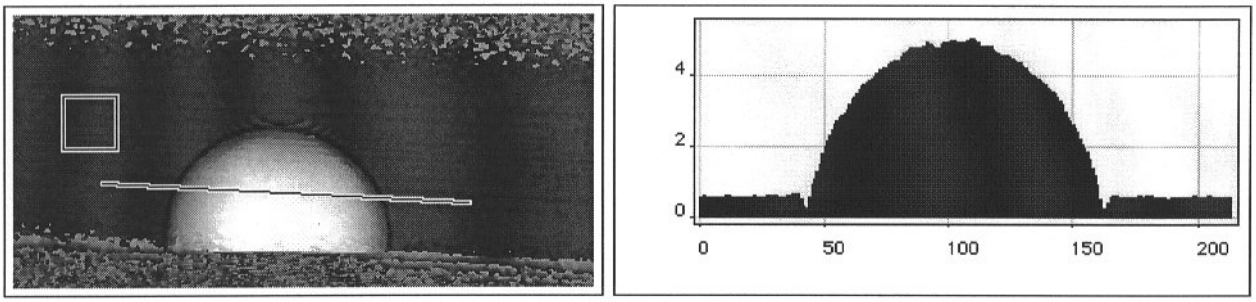

Figure 8. Phase image as reconstructed from a single hologram/reference hologram pair of a latex sphere. A linescan across the sphere is displayed on the right. The phase is given in units of π.

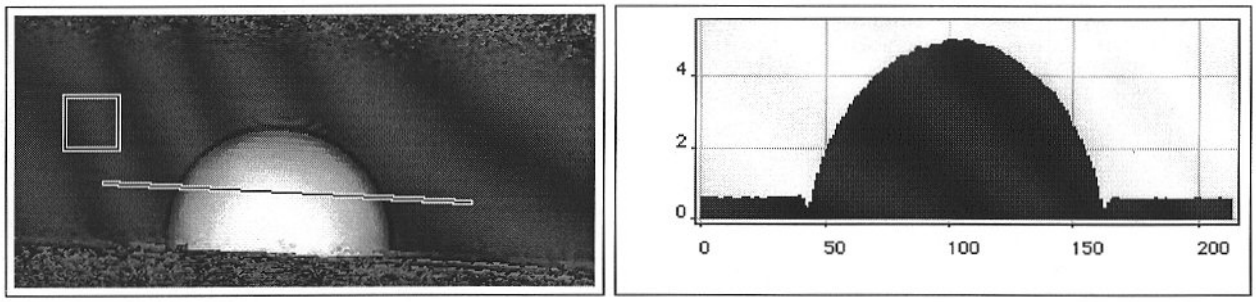

Figure 9. Phase image as reconstructed from a series of hologram/reference hologram pairs shows improved signal/noise ratio. A linescan across the sphere is displayed on the right. The phase is given in units of π.

The 2π ambiguity in the phase image gives rise to so-called "phase-jumps". For example, a phase that increases linearily with x, starting at a phase value of 0.5π, is displayed correctly until the value 2π is reached. Instead of continuing linearily, the phase value jumps down to zero and continues to increases linearily until 2π is reached and the next phase-jump occurs. An example for this behaviour is displayed in Figure 5.

To remediate this problem, i.e., to unwrap the phase image, an automated procedure is desirable, but presently no reliable algorithm appears to be available. Two semi-automated procedures have been developed which are based on the following two different situations.

The first and most simplistic situation is when the actual dynamic range of the phase is ≤2π. As an example, the true phase of an image may range from 0.9π to 2.4π. While the conventional way of displaying this image will result in a phase jump at 2π, this image can easily be displayed without phase-jumps by the following algorithm: subtract X π (with $0 \leq X \leq 2$) from the phase image and then add to all negative pixel values in the image the value of 2π. As a result, the image is still displayed in the [0,2π[range, but the phase jump disappears. This functionality is a very fast, interactive procedure with the phase-offset (-X π in the example) as free parameter which can be modified with the arrow keys on the keyboard. It should be noted that this procedure of phase unwrapping is not sensitive to noise in the image. The second, and much more complex, situation is encountered with phase images whose true dynamic range is >2π. Although it is straightforward to come up with an automatic algorithm for phase unwrapping on a noise-free image, real phase images exhibit shot noise, which can be a serious problem for automated procedures. From our experience, semi-automatic phase unwrapping is reasonably fast and presently yields the most reliable results.

The phase unwrapping procedure we have developed is based on the following idea. For reasons of simplicity, we assume that the true dynamic range for an arbitrary phase image is 3π. Therefore, the conventionally reconstructed phase image ϕ_0 must contain phase jumps. From this image ϕ_0 we first create the phase image ϕ_1 according to:

$$\phi_0 = \begin{cases} \phi_0 & \text{for } \phi_0 - \pi \geq 0 \\ \phi_0 + 2\pi & \text{for } \phi_0 - \pi < 0 \end{cases} \qquad (4)$$

The two phase images ϕ_0 and ϕ_1 cover a dynamic range of [0, 2π[and [π, 3π[respectively. Both images carry the same

information, but display phase jumps in different areas, as seen in figures 6a and 6b (important note: the phase values of ϕ_0 and ϕ_1 in some areas are identical, but differ by 2π in other areas). The phase jumps in ϕ_0 are eliminated by selecting a rectangular area $((x_1, y_1);(x_2,y_2))$ in ϕ_0 that contains a phase jump and replacing it by the area with identical coordinates $((x_1, y_1);(x_2,y_2))$ in ϕ_1. In this way, all phase jumps in ϕ_0 can be removed. For images with many phase jumps, i.e., a (true) dynamic range of $>3\pi$, the procedure is simply an extension of the procedure discussed.

Computer/Remote Control

Working with live-time images, image processing and digital image storage (over the network) eliminates the need for the dark room [13] and lays the ground work for computer-assisted procedures on the microscope. Just as the autoalignment package [5] simplifies the task of the fine tuning of the electron microscope, many tasks in the everyday application of holography can also be simplified. The first software plug-in that would allow many parameters of the Hitachi HF-2000 to be controlled from the scripting level was written in (W.J. deRuijter, personal communication, 1993). At that time, one of our interests was to simplify the task of switching between the standard microscopy mode and the holography mode by using menu items. Later on, even an automatic alignment for holographic fringes was established [3]. The software was subsequently rewritten (M. Lehmann, personal communication, 1994) to the point where all digitally functions available via the RS232 interface of the HF-2000 were accessible from a scripting level.

While more and more automated procedures are being created, the software package TimbuktuPro (by Farallon; now Netopia, Alameda, CA) opened a completely new route to the remote control of instruments. This software package permits the screen contents and the mouse and keyboard functionality of a local computer (the computer at the microscope) to be mirrored by a remote computer. Provided with a fast connection (T1 or better), the operator can physically be far away from instruments but still control the instrument as if sitting at the local computer [2, 9].

Holography and Computer Control

One of our most recent efforts addresses the improvement of the signal-to-noise ratio in the reconstructed phase and amplitude images. As discussed in [4, 6, 12], taking a reference hologram together with the normal hologram is important to remove artifacts. Therefore, the phase shifting technique described in [7] is not used in our effort.

On an ideal microscope, the signal-to-noise ratio of phase and amplitude images is increased by increasing the exposure time, while keeping the illumination conditions constant. However, instrumental instabilities limit this approach for the every-day use.

In general, any drift of the interference pattern while recording diminishes the contrast of the fringes, thus decreasing the signal-to-noise ratio in the reconstructed images. Any drift between the recording of the hologram and the reference hologram causes a re-appearance of the Fresnel fringes of the biprism. In Figure 7, the image phase of half a latex sphere is shown. The remanent Fresnel fringes in the field- and specimen-free area are unwanted artifacts and indicate that the interference pattern was drifting.

While the exposure time for each hologram depends on the momentary overall stability of the microscope and is not directly controlable, the time delay between recording the hologram and reference hologram can be minimized by automation (in our case $\approx$4 sec down to <0.5 sec). For this, a procedure was set up using both our microscope control and reconstruction techniques. In the first part of the procedure a short interactive calibration determines the magnitude and direction for moving the sample in and out of the interference pattern. In the second part of the procedure, the computer records the hologram, moves the specimen out of the interference area, records a reference hologram and moves the sample back into the interference area. The procedure continues to record additional "hologram pairs", until the operator intervenes. In the third part of the procedure, the complex images from all hologram pairs of the series are reconstructed, once the reconstruction procedure (defining type and size of aperture and final image size) for the first hologram pair is established.

In order to combine the information present in each reconstructed complex image, we used a cross-correlation to determine the offset between images, but found this procedure unsatisfactory in some cases, where the existence of Fresnel fringes of the biprism dominates object features. A semiautomatic process, however, yields satisfactory results under nearly all conditions, and is based on the following considerations. We refer to all images of the series as $S^1(x_m, y_n)$, ..., $S^l(x_m, y_n)$, where l is the number of all images in the series. Each of these images can be offset by Δm, Δn with respect to its own origin. By varying interactively Δm, Δn in the following expression:

$$\arctan 2\left\lceil \frac{\Re\left[S^l(x_{m+\Delta ml}, y_{n+\Delta nl}) / S^1(x_m, y_n)\right]}{\Im\left[S^l(x_{m+\Delta ml}, y_{n+\Delta nl}) / S^1(x_m, y_n)\right]} \right\rfloor \quad (5)$$

and viewing the result, the object of interest will disappear for the true choice of $(\Delta m_l, \Delta n_l)$. This procedure is quite fast and yields excellent results. As an example of this method, we have recorded a series of holograms with l = 5. Figure 8 displays the reconstructed phase from the first

reconstructed image of the series, arctan2 [$\Re(S^1) / \Im(S^1)$]. A linescan across the sphere is shown on the right-hand side. Figure 9 shows the reconstructed phase from the entire series ($\Sigma S^l (x_{m+\Delta ml}, y_{n+\Delta nl})$), and a linescan across the sphere (corresponding to the linescan in Figure 8) is displayed on the right-hand side. The signal-to-noise ratio is clearly improved by our process. To verify the findings, the standard deviation in each of the squares of Figures 8 and 9 was evaluated. For the area in figure 8 we have found $\sigma = 1.94 \pm 0.14$, whereas the same area in Figure 9 yields $\sigma = 1.99 \pm 0.068$, which is to be expected if we assume a similar signal-to-noise ratio in all holograms of this series.

Conclusion

Computer automation of transmission electron microscope (TEM) operating procedures simplifies not only routine tasks at the microscope but also allows the implementation of functionalities and features that are tedious to perform on an every day basis (e.g., microscope alignments, recording a series of electron holograms and their reference holograms, and hologram reconstruction). In addition, automated procedures can easily include routines that keep track of microscope settings, processing steps and many other details that are retained with each recorded or processed image. Automated procedures for electron holography allow to record several holograms with their respective reference holograms, thereby improving the signal-to-noise ratio in phase images.

We believe that one of the most important features of our present set-up is the use of a scripting language. Both the microscope and camera control as well as many image processing and handling tools are available on a scripting level. Not only has the scripting language simplified the creation of routines for holography, but also ensures that these and other routines can be adapted easily to the changing needs for electron microscopy.

Acknowledgements

Research sponsored by the Assistant Secretary for Energy Efficiency and Renewable Energy, Office of Transportation Technologies, as part of the High Temperature Materials Laboratory User Program, Oak Ridge National Laboratory, managed by Lockheed Martin Energy Research Corp. for the U.S. Department of Energy under contract number DE-AC05-96OR22464.

References

1. Ade G, Lauer R (1991) Exponentialfilter zur Verringerung des Rauschens in Rekonstruktionen von off-axis-Hologrammen (Exponential filter for noise reduction in reconstructions of off-axis holograms). Optik **88** (Suppl 4): 96.

2. Cross-Country Characterization of Materials (1996) Adv Mater Processes **150**: 4.

3. DeRuijter WJ (1994) Utilization of slow-scan CCD cameras for quantitative electron holography. MSA Bull **24**: 451-458.

4. DeRuijter WJ, Weiss JK (1993) Detection limits in quantitative off-axis electron holography. Ultramicroscopy **50**: 269-283.

5. Krivanek OL, Fan GY (1992) Complete HREM autotuning using automated diffraction analysis. Proc Ann Meeting Microsc Soc America. Bailey GW, Bentley J, Small JA (eds). San Francisco Press, San Francisco. Part 1, pp 96-97.

6. Rau WD, Lichte H, Voelkl E (1991) Real-time reconstruction of electron off-axis holograms recorded with a high pixel CCD camera. J Comput Assist Microsc **3**: 51-63.

7. Ru Q (1995) Phase-shifting techniques in electron holography. In: Electron Holography. Tonomura A, Allard LF, Pozzi G, Joy DC, Ono YA (eds). Elsevier Science BV, Amsterdam. pp. 55-68.

8. Russ JC (1992) The Image Processing Handbook. CRC Press, Boca Raton, FL. pp. 194-202.

9. Voelkl E (1996) Imaging needs for electron microscope distance learning and remote operation. Adv Imaging, Oct 1996, pp 31-33.

10. Voelkl E, Allard LF (1994) Digital processing of high resolution electron holograms. MSA Bull **24**: 466-471.

11. Voelkl E, Lenz F, Fu Q, Lichte H (1994) Density correction of photographic material for further image processing in electron microscopy, Ultramicroscopy **55**: 75-89.

12. Voelkl E, Allard LF, Frost B (1995) A software package for the processing and reconstruction of electron holograms. J Microsc **181**: 39-50.

13. Voelkl E, Allard LF, Dodson TA, More KL, Nolan TA (1996) Digital image acquisition, processing, output and networking in the modern electron microscopy laboratory. Hitachi Instrument News, Electron Microscopy Edition **29**: 5-11.

Discussion with Reviewers

G. Pozzi: It is stated in the paper that the software finds the center of the sideband and centers the reconstruction aperture on it. I suppose that the sideband center is identified with its maximum. If this is true, the method works satisfactorily if a large part of the interference field used in the reconstruction is unperturbed. However, in the case of long range electromagnetic fields, where the whole interference field is perturbed, the above choice is arbitrary and may lead to a wrong phase. Let us consider for example

the case of a constant field, which deflects the electrons and introduces a linear phase term. The corresponding diffraction image or Fourier transform is rigidly displaced and when the aperture is centered on its maximum, the original linear term disappears completely in the reconstruction. As this linear phase can be detected experimentally by means of double exposure electron holography, how do you think with this problem?

Authors: We strongly discourage all of our users to record holograms without a reference hologram. The reconstruction procedures of HoloWorks are therefore split in two parts, with- and without reference hologram. Reconstruction without reference hologram is recommended for preview purposes. When reconstructing a hologram for evaluation, the full reconstruction process includes the reference hologram and finds the position of the sideband from the reference hologram. The reconstruction process supplied by HoloWorks is therefore highly reliable.

If no long range electromagnetic fields are observed, the reconstruction process that includes the reference hologram also removes Fresnel fringes in the vacuum. This last feature is not available from the double exposure technique. Therefore, when using CCD cameras, there appears to be no need to implement the double exposure technique.